

## RECEIVER OPTIMIZATION FOR AN ETENDUE CONSERVING COMPACT LINEAR FRESNEL

Rungasamy AE., Craig KJ\* and Meyer J.P.

\*Author for correspondence

Department of Mechanical and Aeronautical Engineering,  
 University of Pretoria, Pretoria, 0002, South Africa,

E-mail: [ken.craig@up.ac.za](mailto:ken.craig@up.ac.za)

### ABSTRACT

A Compact Linear Fresnel model can be optically optimized at two critical stages; the collector stage and the receiver stage. On the collector side, the mirror field can be designed according to the nonimaging optics principle of Etendue Conservation. The position and size of the mirror field is varied in order to create a system with minimal optical losses. This substantially increases the incident radiation and concentration of the receiver cavity, however the final absorbed radiation of the receiver pipes is dependent on the internal geometry of the receiver itself. Therefore, an optimization study was conducted on the internal geometry of a receiver paired with an enhanced mirror field. The receiver geometry included a parabolic secondary concentrator at the back of the receiver in order to reflect any missed rays. The optimization consisted of two objective functions; namely to maximize absorbed radiation on the receiver pipes and minimize standard deviations on the pipe surface. The results aligned well with theoretical optic calculations in terms of the expected focal point of the collector field and secondaries.

### INTRODUCTION

Linear Fresnel reflector (LFR) technology is a line focus model within the concentrated solar power field. While LFR technology is cheap and easy to maintain, it generally has lower associated efficiencies. This is largely due to the optical losses associated with a discontinuous mirror field [1], as adjacent mirrors block and shade radiation from reaching the receiver. A compact linear Fresnel plant was found to reduce this blocking and shading effect by using a multiple target system, so that adjacent mirrors now lay at dissimilar angles in the central region where most losses occur [2]. It was further found that employing concepts of non-imaging optics could significantly increase the amount of absorbed radiation on the receivers, by designing a mirror field that minimises losses by varying the position and size of the mirrors in the field [3,4]. Etendue is an optical property that represents the product of the area of the source and the solid angle that the systems entrance pupil subtends. Etendue is conserved in a system with zero optical

losses; therefore using etendue conservation as an objective is analogous to minimizing the optical losses in a system [3,5]. However, it should be noted that these increases in absorbed radiation are subject to internal geometry changes in the receiver. Therefore the purpose of this study is to optimize the receiver that is coupled with an Etendue Conserving Compact Linear Fresnel collector field [4]. Additionally, with higher concentrations of incoming radiation, the receiver pipes are more prone to unequal radiation distributions causing undesirable thermal stresses therefore a multi-objective optimization is performed.

### NOMENCLATURE

$U_0$	[m <sup>2</sup> sr]	etendue of incoming radiation
$U_1$	[m <sup>2</sup> sr]	etendue of reflected radiation to receiver 1
$U_2$	[m <sup>2</sup> sr]	etendue of reflected radiation to receiver 2
$\alpha$	[°]	angle of the curve
$\phi$	[°]	angle from point on mirror curve to receiver
$\vartheta$	[°]	receiver angle
$\beta$	[°]	sun angle
$x$	[m]	x-coordinate for parabola
$y$	[m]	y-coordinate for parabola
$H$	[m]	height of the receivers
$D$	[m]	width of the mirror field
$d$	[m]	pipe depth
$p$	[m]	pipe pitch
$R$	[-]	receiver target
$P$	[m]	point along the etendue conserving curve
$r$	[m]	vector from point on the curve to receiver target
$dl$	[m]	infinitesimal length along the etendue conserving curve
$\varepsilon$	[-]	emissivity of surface
$T$	[K]	temperature
Subscripts		
$1,2$		Receiver target
$c$		Centre
$o$		Outer
$p$		Turning point of the parabola

### PARAMETERIZATION OF GEOMETRY

The collector field is designed with etendue conservation as the objective. The governing equation for the curve of the mirror field is

$$dU_0 = dU_1 + dU_2$$

$$\cos \alpha = \cos(\phi_1 - \alpha) + \cos(\phi_2 + \alpha)$$

which is defined in Figures 1 and 2.

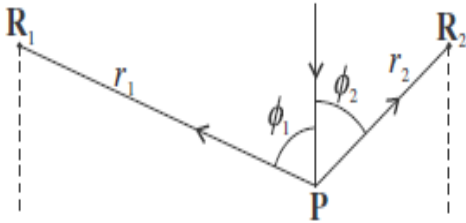


**Figure 1** Schematic representation of the angles between the starting point P and the two receivers [3]

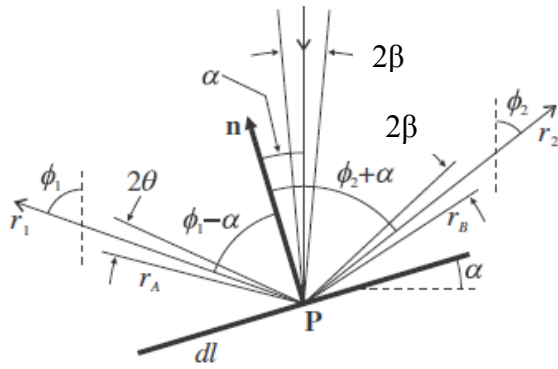


**Figure 2** Etendue balance diagram for light reflected to two receivers over length dl [3].

The resultant curve is then discretized in order to create a physical mirror field with a single target section consisting of the mirrors closest to the receivers and a multiple target section in the centre of the mirror field [4].

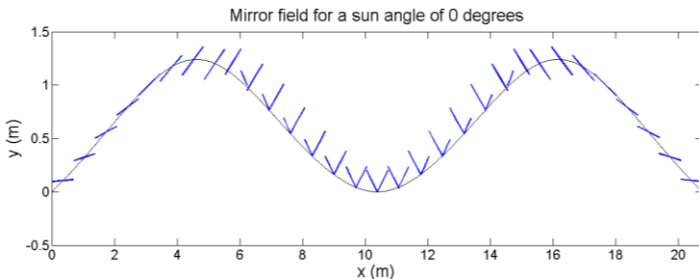


**Figure 3** Discretized peak mirror field [4]

Line focusing receivers are often trapezoidal in shape, with secondaries varying in design [6]. The receiver in this study contains four pipes used for a once through system, a compound parabolic secondary concentrator on the back wall

and fully reflective coatings on the receiver cavity walls. The collector field targets two focal points corresponding to the two receiver centre points of (0,6) and (20.7681,6). The secondary concentrator then reflects any missed rays back onto the focal point of the parabola that lies along the receiver pipes centre line, in between the outer receiver pipes (0.1m away from the collector focal point).

The equation for the secondary concentrators is calculated based on the focal point and turning points, for example the equation for secondary concentrator 1 is

$$y = -2.831(x - x_p)^2 + y_p \text{ with } y_p = 6.11661$$

**Table 1** Parameterized internal receiver geometry

Parameter	Symbol	Minimum value	Maximum value	Fixed values
Pipe depth	$d$ [mm]	0.04	0.1517	-
Outer pitch	$po$ [mm]	0.065	0.09	-
Centre pitch	$pc$ [mm]	0.065	0.125	-
Receiver angle	$\theta$ [°]	30	75	-
Aperture		-	-	1
Glass thickness		-	-	0.008

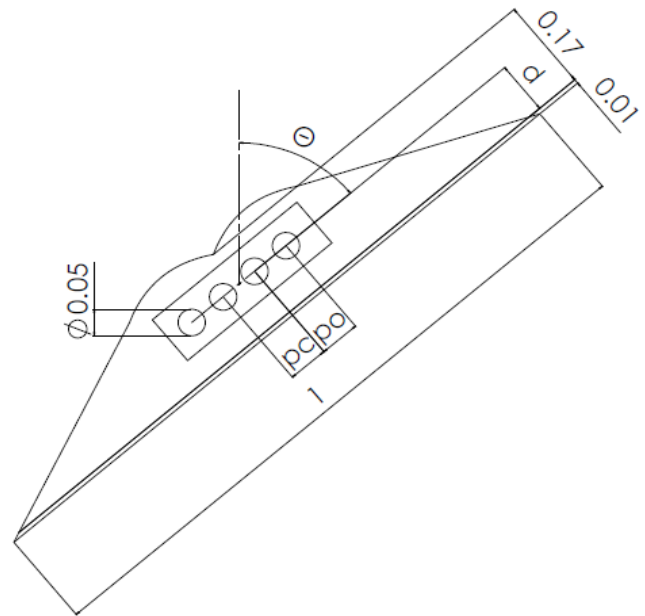


**Figure 4** Compound parabolic secondary receiver parameterized geometry

Four parameters are optimized (listed in Table 1 and displayed in Figure 4); the central pipe pitch, outer pipe pitch, pipe depth and receiver angle. The parameters varied are not constrained, however the upper bound of the receiver depth and pipe outer pitch are limited based on feasible physical designs.

A smaller optimization study was done on the aperture size and the results confirm that an oversized aperture can increase

the amount of incident radiation and concentration values. A large aperture is then used for the subsequent optimization, along with standard industry thicknesses for glass in Linear Fresnel receivers.

### DOMAIN AND BOUNDARY CONDITIONS

The compact linear Fresnel receiver model was created using two dimensions and solid phase materials. ANSYS Fluent v15.0 was used to create a finite volume model that performed the same function as a ray tracing software such as SolTrace.

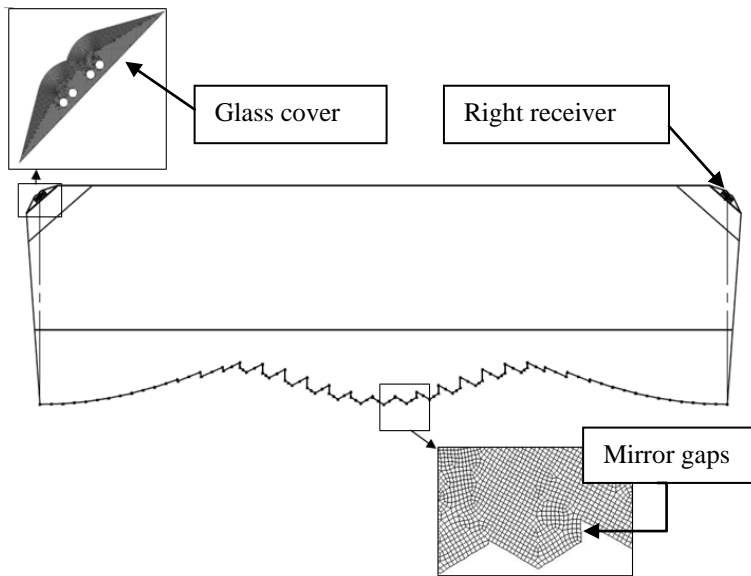


**Figure 5** Domain and boundary conditions for 2D CFD model

The domain (see Figure 5) consists of the collector field, the open air domain and two trapezoidal receivers with a glass cover on the front. Ideal conditions were placed on the reflective and absorptive boundaries and the glass cover on the receiver has a refractive index of 1.5. When modelling absorption through the glass it was found to significantly reduce the sensitivity of the absorbed radiation flux to internal geometry changes and therefore no absorption coefficient was used for the optimization study. This ultimately restricted heat transfer in the model, in order to better isolate the effects of the incoming radiation on the system.

**Table 2** Boundary conditions for the 2D CFD model

Named selection	2D Boundary condition
Radiation source	Specular radiation of $1000\text{W/m}^2$ with a beam angle of $0.53^\circ$
Collector pipes	Fixed temperature $\varepsilon = 1$ , $T = 1.0\text{K}$ .
Receiver cavity walls	Fixed temperature $\varepsilon = 0$ , $T = 1.0\text{K}$
Transparent cover outer wall	Semi-transparent, coupled wall
Transparent cover	Semi-transparent, coupled wall

inner wall	
Mirrors	Fixed temperature, specular reflection $\varepsilon = 0$ , $T = 1.0\text{K}$
Mirror gaps and edges of domain	Fixed temperature $\varepsilon = 1$ , $T = 1.0\text{K}$ .

### CFD MODELLING

A corresponding study was completed in SolTrace to validate the use of the finite volume method for ray tracing, along with a number of test cases on simpler geometries [7]. The finite volume method can yield accurate answers, however for coarser settings it is subject to false scattering and it is therefore imperative to use a fine mesh and radiation discretization setting. A mesh and discrete ordinates sensitivity study was subsequently performed to establish the settings required for mesh and discrete ordinate independence.

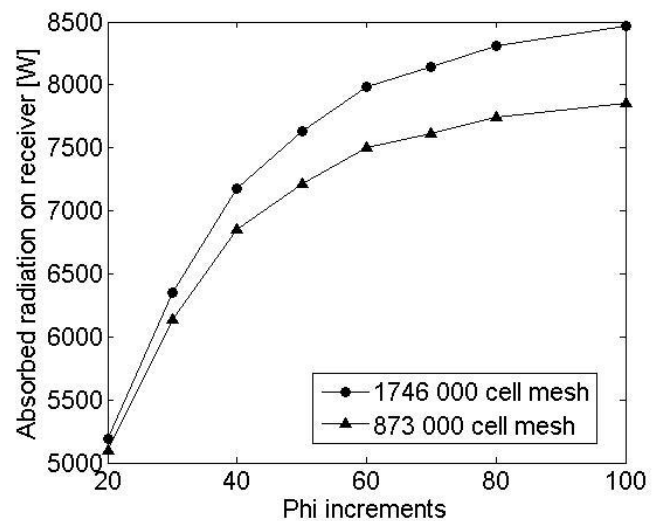


**Figure 6** Graph of discrete ordinates discretization settings versus absorbed radiation on receiver pipes

In two dimensions, radiation can be modelled using different settings for the theta and phi discretizations, because only 3 divisions are required in the third dimension if the global coordinate system is chosen appropriately. This significantly reduces the computing time associated with what would otherwise be a relatively fine discrete ordinates setting. For the discrete ordinates study, the number of theta discretizations is fixed at 3 while the number of phi discretizations varies, with the pixelations for both fixed at 3. The resultant phi discretization that is used for the optimization is 60 for a mesh with approximately a million cells. While the most accurate settings would be for a discretization of approximately 500, it is found that the absorbed radiation was dependent on the discretization in a predictable way and the above setting was sufficient for predicting geometrical optimization changes. This meant that, in addition to the energy equation, a further  $4 \times 3 \times 60 = 720$  differential equations were solved in the discrete ordinates implementation of the Radiation Transport Equation.

The mesh (see inserts in Figure 5) used for the optimization has a face sizing of 0.002 in the receiver cavity and in the glass, 0.01 in the receiver adjacent air, 0.03 on the mirror adjacent domain and 0.05 in the central air section. A quad mesh was used and the refinement was constructed according to sections where the direction of the incoming radiation is most important.

Two objective functions were used in the receiver optimization; the first objective was to maximize the total absorbed radiation on the receiver pipes. The second objective was to minimize the standard deviation of absorbed radiation on the surface of the pipes, which serves to reduce hot spots and associated thermal stresses. The ideal candidate point was therefore one with a very high amount of absorbed radiation evenly distributed around the pipe.

DesignXplorer in ANSYS Workbench was used to run a response surface optimization, which uses the Central Composite Design method to create the design points for the response surfaces.

### CFD RESULTS

The results obtained from the simulations (Figures 7 and 8) illustrate that the incident radiation peaks on the two receivers are symmetrical but show that the peak incident radiation does not necessarily lie at the predicted focal point. This is due to the refraction of the incoming radiation through the glass layer.

The receivers shadow the mirror field directly below it and there are some missed rays in the centre of the field (Figure 7). It is therefore not a zero loss collector field however there is a significant increase in the amount of incident radiation on the receiver when using this etendue-matched collector field.

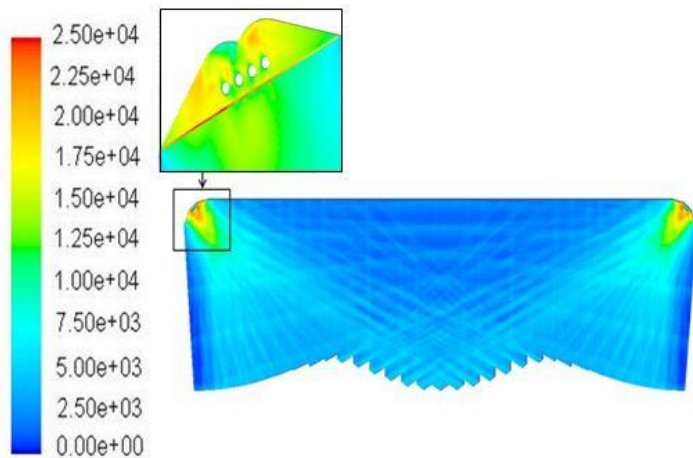


**Figure 7** Incident radiation contour for 2D CFD modelling

### OPTIMIZATION RESULTS

The optimization results listed in Table 3 were obtained for the multi-objective optimization.

**Table 3** Optimized parameter results

Parameter	Optimized value
Pipe depth [mm]	0.04
Outer pitch [mm]	0.125
Centre pitch [mm]	0.065
Receiver angle [°]	45

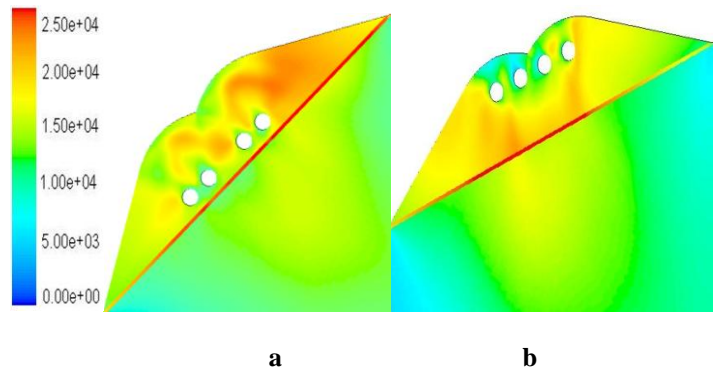


**Figure 8** Incident radiation contours of receiver for a) optimum and b) sample design points

For the majority of the parameters, the resultant design points lie on the limit of their prescribed ranges. However, as displayed in Figure 9, the optimum receiver angle was approximately 45°, which corresponds to the centre of the receiver being pointed towards the centre of the collector field.

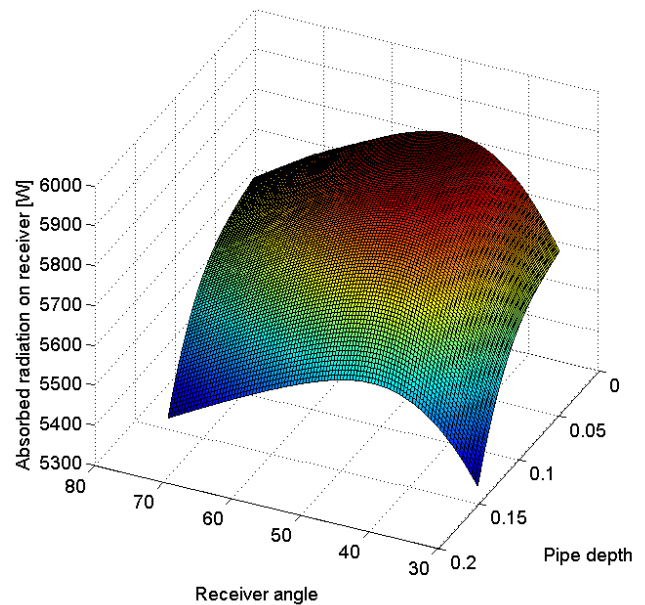


**Figure 9** Response surface of absorbed radiation on receiver pipes versus receiver angle and pipe depth

The receiver angle that points towards the middle of the field, allows for radiation from the further side of the multiple mirror target section to reach the aperture, thereby increasing the amount of absorbed radiation on the receiver pipes. The optimum pipe depth is as close to the aperture as possible, despite the predicted focal point of the secondaries lying very close to the back of the receiver cavity. This is also due to the fact that the receiver pipes block the secondary reflective surfaces when located close to the back of the cavity. The sensitivity study associated with the multi-objective optimization identified the pipe depth as the parameter that caused the most variation in the total absorbed radiation.

and absorbed radiation, limited only by physically feasible geometry constraints. The pipe pitch yields a result that places the pipes closer to the secondary focal point than the collector focal point, which suggests that if the incoming radiation passes between the centre pipes it is reflected by the secondary.

Therefore the resultant receiver distribution is the one that prioritises intercepting incoming radiation close to the glass cover, while arranging the pipe pitch such that blocking on the secondary is minimized. This increases overall radiation but also reduces standard deviations of absorbed radiation along the circumference of the individual pipes themselves, but also between the receiver pipes.

In Figure 11b, it can be seen that there is variation in the absorbed radiation on the receiver pipe, with the peaks occurring on the portions of pipe that are facing the collector field. The direct incoming radiation is therefore the dominant mode of radiation absorption. This is partly due to the fact that the collector field is targeted at a focal point between the pipes as opposed to along the secondary. The outer pipes also show a high amount of absorbed radiation from the sides of the pipe, though there is a degree of asymmetry between the outer pipes. This indicates that there is more incoming radiation towards the top of the receiver.

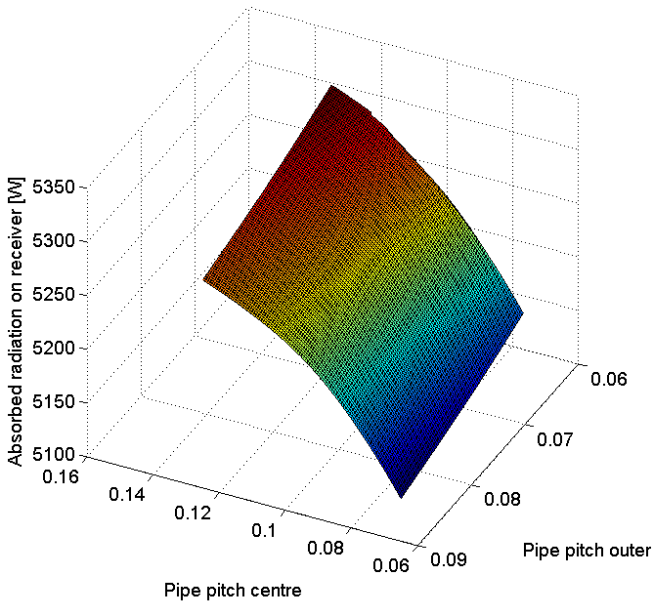


**Figure 10** Response surface of absorbed radiation on receiver pipes versus centre pipe pitch and outer pipe pitch

The response surface for pipe pitch variation (Figure 10) contains a peak that lies on the extremum. This effectively means that there is a direct correlation between the pipe pitch

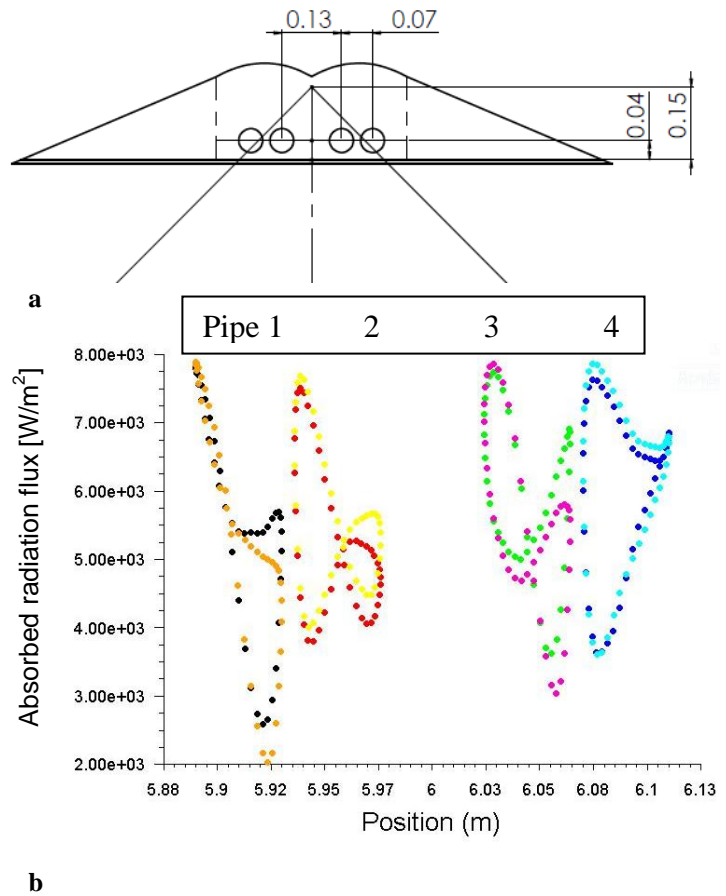
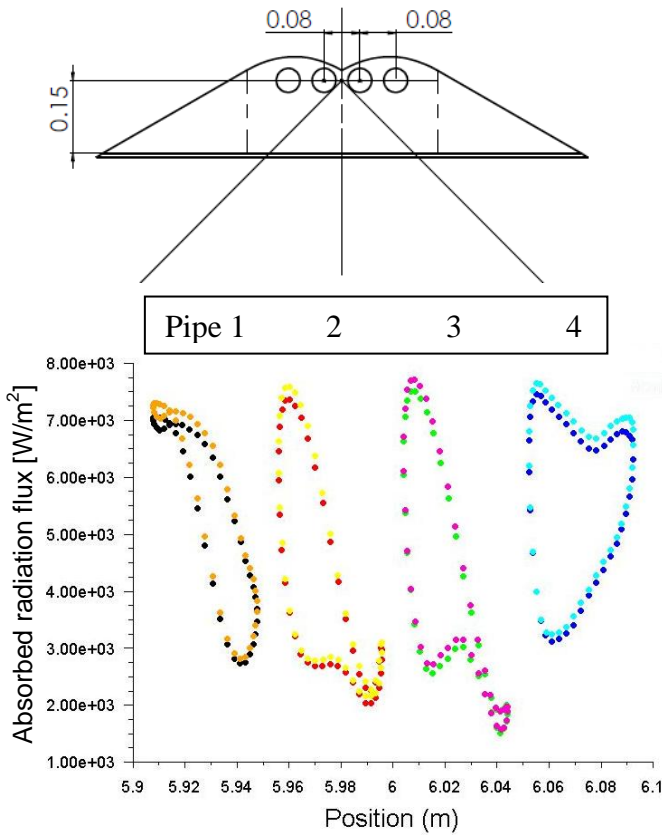


**Figure 11a** Optimized receiver geometry and associated focal points and **b** Resultant absorbed radiation on receiver pipes

**Table 4** Comparison of optimum point and sample point

	Sample Point	Optimum point
Parameters	$d = 0.1352$ , $\Theta = 68.3^\circ$ , $p_o = 0.075\text{m}$ and $p_c = 0.075\text{m}$	$d = 0.04$ , $\Theta = 45^\circ$ , $p_o = 0.065\text{m}$ and $p_c = 0.125\text{m}$
Total absorbed radiation [W]	5213	5721.14
Total standard deviation [W/m <sup>2</sup> ]	2323.95	1351.99

There is a small amount of asymmetry when the parameters were created for each receiver and this is due to false scattering and ray effects. However the response surfaces all yield the same trend in parameter variation.

While the optics study suggests that a large aperture and pipes close to the glass cover were best, thermal studies [8] suggested that the convective losses from the front of the receiver drive the receiver geometry towards a small aperture and pipes near the back of the cavity. There is therefore a necessary trade-off to be made between designing a system to ensure the maximum absorbed radiation occurs on the receiver pipes and limiting the thermal re-radiation and convective losses that occur when conjugate heat transfer is modelled.

## CONCLUSION

It was found that the resultant pipe pitch dimensions correspond to the predicted focal points in a longitudinal direction, however they are much closer to the transparent cover than the focal point predicted. This allows for a more uniform distribution of radiation around the pipe circumference as any rays that miss the receiver pipes will be reflected back onto the secondary focal points. This is due to the high levels of blocking experienced by the secondary when the pipes are moved back in the receiver cavity. When the receiver pipes are moved forward and apart from the centre, the receiver geometry is better utilised for incoming radiation at several different angles. It should be noted that a potential alternative could be to target the secondary itself with some of the mirrors rather than aiming all the mirrors at the pipes themselves. This strategy also allows for larger tolerances on the receiver targeting [9,10].

Optimizing the receiver geometry is the necessary optical progression once the etendue conserving compact linear Fresnel system had been designed. The resultant receiver geometry has a higher total absorbed radiation and lower standard deviation. It should be noted however, that the results of the optical optimization are very different to that of a thermal optimization which would include factors such as the changing steam volume fraction of the heat transfer fluid in the receiver pipes and the varying internal and external heat transfer coefficients; therefore future studies will take both into consideration with a three dimensional model.

## ACKNOWLEDGEMENTS

The authors would like to acknowledge the support from the University of Pretoria (South Africa) and the South African National Research Foundation (DST-NRF Solar Spoke).

## REFERENCES

- [1] Walker, G., Von Backström, T.W., and Paul Gauché. A Method of Increasing Collector Aperture in Linear Fresnel Solar Concentrators at High Concentrators at High Zenith Angles, *Proceedings of the Southern African Solar Energy Conference*, Stellenbosch, South Africa, 2012
- [2] Mills, D.R. and Morrison G.L., Compact Linear Fresnel Reflector Solar Thermal Powerplants. *Solar Energy*. Vol. 68, No. 3, 2000, pp263-283
- [3] Chaves, J., Collares-Pereira, M., Etendue-matched two-stage concentrator with multiple receivers. *Solar Energy*, Vol. 84, 2010, pp196-207.
- [4] Rungasamy A.E., Craig, K.J and Meyer J.P., 3D CFD modelling of a slanted receiver in a compact linear Fresnel plant with etendue-matched mirror field, *Proceedings of the SolarPaces Conference*, Beijing, China, 2014.
- [5] Chaves, J., Collares-Pereira, M., 2009. Primary concentrator with adjusted etendue combined with secondaries associated to multiple receivers and with convection reduction, *International patent application* PCT/PT2009/000026
- [6] Cooper T., Ambrosetti G., Pedretti A. and Steinfeld A.. Theory and design of line-to-point focus solar concentrators with tracking secondary optics. *Applied Optics*, Vol. 52, No. 35, 2013, pp8586-8616
- [7] Moghimi, M.A., Craig, K.J. and Meyer J.P., A novel computational approach to the combined optical and thermal modelling of a linear Fresnel reflector receiver, *Southern African Solar Energy Conference 2015*, 11-13May 2015, Kruger National Park, South Africa.
- [8] Pye, J.D., System Modelling of the Compact Linear Fresnel Reflector. *PhD Thesis*. Australia: University of New South Wales, 2008.
- [9] Canavaro D, Chaves J. and Collares-Periera M. Infinitesimal etendue and Simultaneous Multiple Surface (SMS) concentrators for fixed receiver troughs. *Solar Energy*. Vol.97,2013,pp493-504.
- [10] Canavaro D, Chaves J. and Collares-Periera M. Simultaneous Multiple Surface method for Linear Fresnel concentrators with tubular receiver. *Solar Energy*. Vol. 110, 2014,pp105-116